

# Global Attention-Guided Dual-Domain Point Cloud Feature Learning for Classification and Segmentation

Zihao Li, Pan Gao, Kang You, Chuan Yan, and Manoranjan Paul

**Abstract**—Previous studies have demonstrated the effectiveness of point-based neural models on the point cloud analysis task. However, there remains a crucial issue on producing the efficient input embedding for raw point coordinates. Moreover, another issue lies in the limited efficiency of neighboring aggregations, which is a critical component in the network stem. In this paper, we propose a Global Attention-guided Dual-domain Feature Learning network (GAD) to address the above-mentioned issues. We first devise the Contextual Position-enhanced Transformer (CPT) module, which is armed with an improved global attention mechanism, to produce a global-aware input embedding that serves as the guidance to subsequent aggregations. Then, the Dual-domain K-nearest neighbor Feature Fusion (DKFF) is cascaded to conduct effective feature aggregation through novel dual-domain feature learning which appreciates both local geometric relations and long-distance semantic connections. Extensive experiments on multiple point cloud analysis tasks (e.g., classification, part segmentation, and scene semantic segmentation) demonstrate the superior performance of the proposed method and the efficacy of the devised modules.

**Impact Statement**—The 3D point cloud is a fundamental data structure utilized in a wide range of applications, such as intelligent manufacturing, automatic driving, robot control, etc. The efficacy of these applications fundamentally depends on their ability to accurately capture and understand the geometric information of the point cloud data. While most existing methods tend to use complex and expensive frameworks to enhance the understanding ability of the neural model, we propose a simple and cost-efficient method for better information extraction. Experiments show that the proposed method demonstrates state-of-the-art performance with the adaptable traits present in the proposed modules, which has the potential to aid in other point cloud analysis tasks (e.g., completion and compression). In addition, our fully armed method demonstrates a 4% improvement in classification compared to the baseline in the ablation study, marking a significant leap forward.

**Index Terms**—point cloud, global attention-guided, dual-domain feature learning, classification, segmentation

## I. INTRODUCTION

AS a flexible three-dimensional (3D) data format, point cloud has been widely used in numerous vision applications, including autonomous driving, robotics, medical

treatment, etc. The point cloud is a collection of unconstrained points that effectively represents objects and scenes, which are typically obtained by applying scanning or sampling techniques to the surfaces of the target 3D shape. Each point within the point cloud comprises a coordinate tuple  $(x, y, z)$ , which is treated as the geometry information, and additional attribute information such as color, reflectance, and normal. With the ongoing progress of point cloud acquisition technology [1], [2] and the fast development of 3D vision applications [3], [4], [5], the efficient analysis of point cloud shapes has emerged as one of the key focuses in both industry and academia [6], [7], [8].

### A. Background

To address the challenge of point cloud analysis task, which lies in tackling the unordered and irregular points, the community has developed three categories of techniques: multi-view-based [9], [10], [11], [12], voxel-based [13], [14], [15], [16], and point-based methods [17], [18], [19], [20], [21]. The multi-view-based methods [9], [10], [11], [12] first project the point cloud into 2D images, and then capitalize on conventional 2D techniques to analysis the point cloud shape. The voxel-based methods [13], [14], [15], [16] quantize the input point cloud into a grid-based representation, and utilize 3D convolution or sparse convolution [22] to conduct feature extraction. However, both 2D projection and voxelization destroy the details of the original point cloud, resulting in information losses and performance bottlenecks. In the past few years, point-based methods, represent by PointNet [17], [23], DGCNN [18], and Point Transformer [19], [24], have rapidly garnered extensive attention due to its exceptional capacity in directly processing raw points.

Despite the significant performance advancements of the point-based models, there exists various deficiencies in existing approaches, one of the key issues arises from inefficient input embedding for input point coordinates. Previous works usually follow a bottom-up pipeline that starts from the details and progressively down-samples the skeleton [23], [16], [24]. The Multi-Layer Perceptron (MLP) [17] is used to simply map the original 3D coordinates into higher dimensions at the initial layer without considering global information. However, we argue that integrating global information in the embedding step facilitates the network learning, since it can serve as a guidance to the subsequent local feature aggregations.

Another issue lies in the limited efficiency of neighboring aggregations. Recent research works [25], [26], [27], [28],

This work was supported by the Natural Science Foundation of China under Grant 62272227. (Corresponding author: Pan Gao.)

Z. Li, P. Gao and K. You are with College of Artificial Intelligence, Nanjing University of Aeronautics and Astronautics, Nanjing 211106, China. (pride\_19@163.com, gaopan.1005@gmail.com, youkang@nuaa.edu.cn)

C. Yan is with Creativity and Graphics Lab, George Mason University, Virginia 22030, US. (cyan3@gmu.edu)

M. Paul is with School of Computing, Mathematics, and Engineering, Charles Sturt University, NSW 2678, Australia. (mpaul@csu.edu.au)

[29] typically conduct multi-scale feature aggregation based on built local graphs. However, these local graphs are either constructed by applying K-Nearest Neighboring (KNN) query on 3D spatial domain or high-dimensional feature domain, neglecting the complementary character of different domains. The KNN graph based on spatial domain gathers the points that are spatially related to each other, and the feature-domain graph links points with long-distance semantic relations. Considering the neighboring points at dual domain is able to enhance the neural model’s ability to appreciate both local geometric relations and long-distance semantic connections, which better improves the efficiency of feature aggregations.

### B. Our Approach

To address the above-mentioned issues, we propose a Global Attention-guided Dual-domain feature learning network (GAD). To be specific, we first design a Contextual Position-enhanced Transformer (CPT) module to fully exploits the prior knowledge of the input point cloud shapes, to produce a global-aware input embedding which serves as a guidance to the subsequent aggregations. The devised CPT module is armed with an improved global attention mechanism to best characterize the point cloud shape from the raw input points. Then, the Double K-nearest neighbor Feature Fusion (DKFF) is cascaded to provide efficient feature aggregation by extracting and fusing local graph dynamics that are obtained in both spatial and feature domains. The feature domain focuses on interacting with points that are semantically related without the limitation of distance constraints, while the spatial domain focuses on the points that are spatially related in 3D coordinate space, which facilitates the feature learning for local geometric details. A ResNet-like [30] fashion that considers skip connections crossing the network stem (i.e., the stacked DKFF modules) and branches (i.e., specific modules for classification and segmentation tasks) is adopted in our pipeline to facilitate network learning. We examine the efficiency of the proposed model on multiple point cloud analysis tasks as well as a variety of datasets, including classification on ModelNet40 [31] and ScanObjectNN [32], part segmentation on ShapeNetPart [33], and indoor scene segmentation on S3DIS [34].

The main contributions of this paper can be summarized as:

- We propose the Contextual Position-enhance Transformer (CPT) module which is armed with an improved global attention mechanism, to produce a global-aware input embedding that serves as the guidance to subsequent aggregations and facilitates network learning.
- We propose the Double K-nearest neighbor Feature Fusion (DKFF) module that provides highly effective feature aggregation by conducting novel dual-domain feature learning. It enhances the neural model’s ability to appreciate both local geometric relations and long-distance semantic connections.
- Levering the proposed CPT module for effective global-aware input embedding and DKFF module for dual-domain feature aggregation, our method attains state-of-the-art performance on multiple point cloud analysis

tasks (e.g., classification, part segmentation, and semantic segmentation).

After reviewing related work in Sec. II, we elaborate the proposed method in Sec. III. Experiments are provided in Sec. IV and the conclusion is drawn in Sec. V.

## II. RELATED WORK

### A. Multi-view based Methods

The multi-view based methods first project 3D point clouds into multiple 2D planes, then use 2D image feature extraction and fusion techniques to analysis point cloud shapes. How to aggregate multiple visual features into a discriminative global feature representation is the key challenge. MVCNN [35] is a pioneering work that maximizes the features of multiple views into a global descriptor, but there is a loss of non-maximum element information. MHBN [36] integrates local features via coordinated bilinear pooling. In addition, Yang *et al.* [10] utilize relational networks to mine interrelationships on a set of views and then aggregate them to obtain an overall object representation. View-GCN [37] uses multiple views as graph nodes, and applies local graph convolution, non-local message passing, and selective view sampling to the constructed graph to form a global shape descriptor. However, the transition to a multi-view representation inevitably results in significant loss of original information from the input point cloud data.

### B. Voxel-based Methods

Voxel-based methods usually voxelize the point cloud into 3D grids, and then apply 3D convolutions on the volumetric representation for feature extraction. Wu *et al.* [31] proposed a convolutional deep belief-based 3D ShapeNet to learn the distribution of points in various 3D shapes. But it does not scale well to dense datasets. To this end, OctNet [38] first uses a hybrid grid-octree structure to divide the point cloud to reduce computational costs. Wang *et al.* [39] proposed an Octree-based CNN to send the average normal vector of the sampling model in the finest leaf octagon to the network to achieve shape classification. PointGrid [40] combines point and grid representations, enabling the network to extract geometric details. In addition, Ben-Shabat *et al.* [41] used the 3D modified Fisher Vector (3DmFV) method to represent the three-dimensional grid, and then used the traditional CNN architecture to learn the global representation. Generally speaking, voxel-based models is constrained by the distortion introduced by voxelization step, leading to performance bottlenecks.

### C. Point-based Methods

Point-based methods directly operate on raw point coordinates without additional preprocessing steps, which can be roughly divided into four representative types: point-based MLP, convolution-based, graph-based and attention-based methods.

1) *Point-based MLP Methods*: Such methods mainly use multiple shared multi-layer perceptrons to model each point independently. As a pioneering work, PointNet [17] applies a shared multi-layer perceptron to each independent point, and then uses a symmetric aggregation function to aggregate global features, which perfectly adapts to the disorder of the point cloud but ignores the connection with surrounding points. Subsequent PointNet++ [23] uses PointNet hierarchically to capture fine geometric structures from the neighborhood of each point. In addition, Duan *et al.* [42] proposed a Structural Relational Network (SRN) using MLP to learn structural relational features between different parts.

2) *Convolution-based Methods*: Unlike fixed convolution kernels for 2D images, convolution kernels for 3D point clouds are difficult to design due to the irregularity of point clouds. RSCNN [43] implements convolution by learning the mapping from low-level relations such as Euclidean distance and relative position between points in the local subset to high-level relations. In addition, Thomas *et al.* [44] use a set of learnable kernels as point cloud rigid and deformable Kernel Point Convolution (KPCConv) operators. Whereas in PointConv [45], a clip is defined as a Monte Carlo estimation of a continuously sampled 3D convolution with a convolution kernel consisting of a weighting function and a density function. In addition, PCNN [46] also proposed a 3D point cloud convolution network based on radial basis function.

3) *Graph-based Methods*: Graph-based methods treat each point of the point cloud as a vertex of a graph, and generate directed edges of the graph from neighbors. ECC [47] utilizes filter generation network and maximum pooling to aggregate domain information. However, DGCNN [18] constructs graphs in feature space and dynamically updates between layers. KCNet [48] learns relevant features based on the kernel and calculates the affinity between the kernel and the neighborhood of a given point. There are also methods that define convolution as spectral filtering, implemented by multiplying the signal on the graph with the eigenvectors of the Laplacian matrix. For example, RGCNN [26] treats the entire point cloud as a complete graph and updates the Laplacian matrix at each layer. In PointGCN [49], KNN is used to find neighbors and then Gaussian kernel is used to weight each edge. The convolution filter is defined as a Chebyshev polynomial in the graph domain, and features are captured by pooling.

4) *Attention-based Methods*: With the success of Transformer in the field of natural language processing, it has also been introduced into 3D vision tasks and has been continuously improved. The attention mechanism is mainly to generate and allocate the weights to features or neighboring points. AdaptConv [27] uses the attention mechanism to design an adaptive graph convolution kernel to calculate and distinguish the different contributions of neighboring points to the center point. RandLA-Net [25] uses Cartesian coordinates and point feature splicing to learn spatial weights to complete local feature aggregation. PointANSL [50] utilizes adaptive sampling to propose a local-nonlocal module to capture the local and long-range dependencies of sampling points. PCT [28] adopts the same architecture as PointNet [17], and proposes Offset-Attention to improve the traditional self-attention. And

PT [19] does subtraction between query and key to get the channel attention score of the vector, which greatly improves the performance. In addition, PVT [51] deeply combines the advantages of point-based and voxel-based networks into Transformer, and proposes a local attention module that attains high efficiency and low computational overhead.

#### D. Summary

In summary, multi-view based methods [35], [36], [10], [37] may suffer from information loss during projection, and voxel-based methods [31], [38], [39], [40], [41] face challenges with distortion and scalability. Point-based methods exhibit high flexibility and fidelity by directly operating on raw data, and showcasing advancements equipped with MLP [17], [23], [42], convolution [43], [44], [45], [46], graph [47], [18], [48], [26], [49], and attention [27], [25], [50], [28], [17], [19], [51] mechanisms. Recent attention-based point models, in particular, have shown promising results in 3D vision tasks by effectively capturing local and global dependencies, without any information loss caused by projection and voxelization distortion.

Compared to the prior point-based methods in the field, the key improvements and novelties of the proposed GAD can be highlighted as follows:

- Global-aware input embedding. The CPT module incorporates global information into the initial input embedding, providing a more informative representation that guides subsequent local feature aggregations.
- Improved global attention mechanism. The CPT employs an enhanced attention mechanism to effectively characterize the overall point cloud shape from raw input points, capturing global context.
- Dual-domain feature learning. The DKFF module performs feature aggregation using both spatial and feature domain local graphs, capturing local geometric relations and long-distance semantic connections simultaneously.
- The combination of CPT and DKFF modules enables GAD to achieve superior performance on multiple point cloud analysis tasks, including classification, part segmentation, and semantic segmentation.

### III. METHODOLOGY

We propose a global attention-guided dual-domain feature learning network for point cloud classification and segmentation tasks. This section first outlines the overall network structure and then elaborates the technical details of each module.

#### A. Framework

The network architecture of our proposed method is shown in Fig. 1. We initially characterizes the general geometric features of the input point cloud in the shared stem of the network, then two downstream branches are employed for specific tasks (e.g., classification and segmentation). For ease of expression, we use the term “*stem*” to denote the common feature extraction phase preceding the specialized task branches.

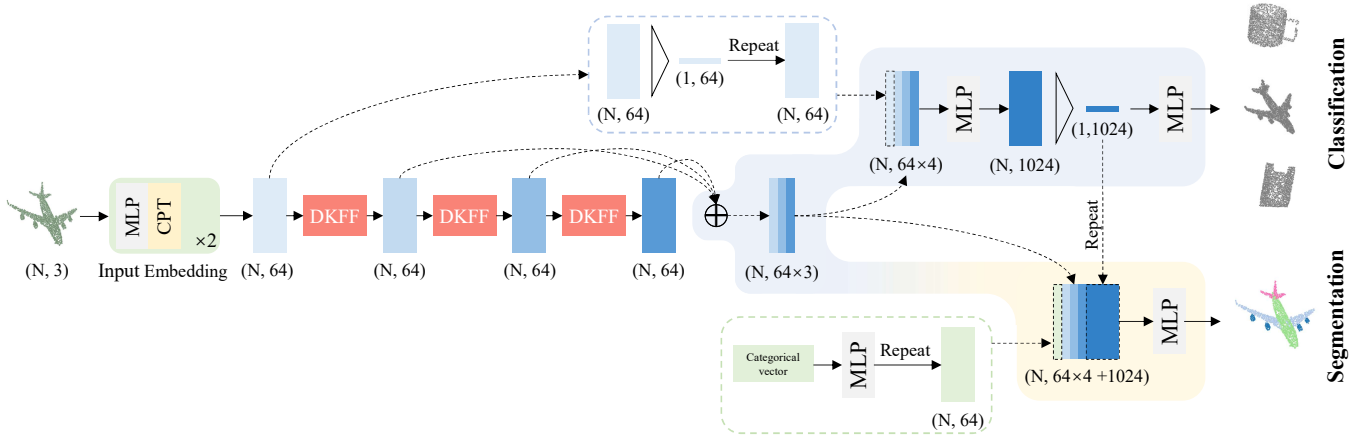


Fig. 1: Network architecture of proposed method. “MLP” refers to the Multi-Layer Perceptron; “CPT” represents the devised Contextual Position-enhanced Transformer module; “DKFF” means the Double K-nearest neighbor Feature Fusion module;  $N$  refers to the number of points of the input point cloud.

1) *Shared Network Stem*: As shown in Fig. 1, we first introduce Contextual Position-enhanced Transformer (CPT) to embed the raw point coordinates into feature space, leveraging a global attention mechanism that efficiently exploits the information of the full point cloud shapes. Based on this, Double K-nearest Feature Fusion (DKFF) modules are cascaded to enhance the obtained global features with locality-aware aggregation in both spatial and feature domains. In this way, the provision of global information from the CPT module serves as guidance for the subsequent dual-domain feature learning, facilitates effective geometric modeling for both global shapes and local details.

2) *Classification Branch*: The features produced by the CPT module incorporating global shape information are aggregated through max-pooling to form a one-dimensional global vector for the initial provision of the global shape context. Then, multi-level features derived from DKFF modules are concatenated and utilized to further enhance and modulate the global vector with additional details.

3) *Segmentation Branch*: Similar to the classification branch, the segmentation branch embraces the integration of global and local features, yet it incorporates a deeper global feature, i.e., the ultimate vector that precedes the classification head in the classification task. In addition, category vector is also concatenated into features as additional messages to the neural model. The concatenated feature, which best describes the geometric information of the input sample, are followed by a multi-layer perceptron that specifies a segmentation label for each point in the point cloud.

### B. Contextual Position-Enhanced Transformer (CPT)

Position encoding is essential for tasks that involve modeling and analyzing the geometry of a point cloud based on its spatial coordinates. Previous works typically utilized a multi-layer perceptron to map three-dimensional coordinates into higher dimensions as the initial features. However, simple mapping techniques do not enable the network to grasp the information of the point cloud geometry due to insufficient

interaction within the point set, leading to ineffective feature aggregations. To address this issue, we develop the Contextual Position-enhanced Transformer (CPT) module to generate effective input embedding with integrated global information that serves as a priori guidance to subsequent feature aggregations.

The detailed structure of devised CPT module is shown in Fig. 2. To be specific, we first define the original input point cloud as  $X = \{x_i | i = 1, 2, \dots, N\} \in \mathbb{R}^{N \times 3}$ , where  $x_i$  represents the three-dimensional coordinates  $(x, y, z)$  of the  $i$ -th point. We use the raw coordinates to obtain the naive position embedding  $P_X$  through the shared MLP, which can be expressed as:

$$P_X = MLP(X) \quad (1)$$

Then, the naive position embedding  $P_X$  is added with the point cloud feature  $F$  to produce the input feature  $F_{in} \in \mathbb{R}^{N \times C}$  for the subsequent attention mechanism. Note that the feature  $F$  of the first CPT module is initialized by a non-linear mapping of the input points, e.g.,  $F = MLP(X)$ .

Next, we devise an attention mechanism that is based on contextual position bias to effectively calculate the semantic similarity among all points in the input point cloud. Different from the previous attention mechanism that directly use the relation calculated by the *query* and *key* as the position bias, we consider a deeper interaction between the position embedding  $P_X$ , *query*, and *key* to get the position bias with abundant contextual information. Specifically, let  $Q_F$ ,  $K_F$ , and  $V_F$  be the *query*, *key*, and *value* matrices that generated by linear transformation on the feature  $F_{in}$  respectively, we calculate the contextual position bias  $bias_X$  as follows:

$$bias_X = Q_F \times P_X^T + K_F \times P_X^T \quad (2)$$

Based on this, the employed attention mechanism can be expressed as follows:

$$F_{sa} = SoftMax\left(\frac{Q_F \times K_F^T + bias_X}{\sqrt{C}}\right) \times (V_F + P_X) \quad (3)$$

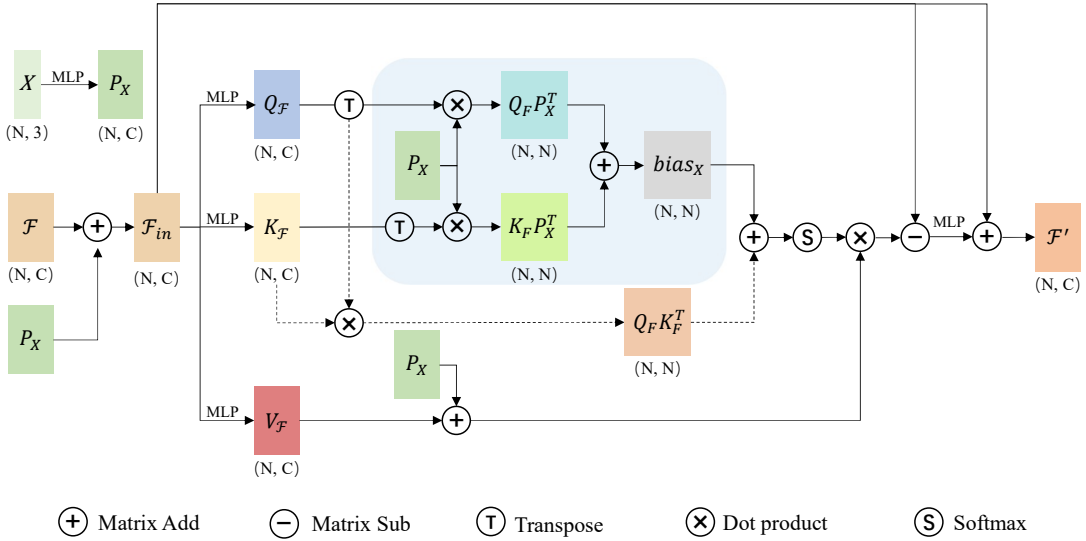


Fig. 2: Proposed Contextual Position-enhanced Transformer (CPT) module.  $X$  refers to the original point cloud coordinates;  $F$  refers to the point cloud features;  $N$  represents the number of points of the input point cloud;  $C$  denotes the dimension of feature channel; MLP means multilayer perceptron.

where  $C$  represents the feature channel dimension;  $F_{sa}$  refers to the feature by the attention mechanism.

Given that  $Q_F$ ,  $K_F$ , and  $V_F$  are derived from the high-dimensional features, employing a conventional attention mechanism directly in this feature space is empirically inefficient, due to the risk of an excessive focus on high-level semantic information and neglect of the shape details. The contextual position bias  $bias_X$  serves as a timely injection of raw point cloud geometry position, effectively supplements detailed information in high-dimensional semantic features.

As the final step, the CPT module adopts the offset calculation between the self-attention features and the input features by subtraction, similar to the scheme used in PCT [28], to obtain better network performance. Mathematically,

$$F' = MLP(F_{in} - F_{sa}) + F_{in} \quad (4)$$

where  $F'$  represents the output of the proposed CPT module.

### C. Double K-nearest neighbor Feature Fusion (DKFF)

The fashion of directly constructing local graphs in the feature domain has been proven to be effective for point cloud analysis tasks, owing to the ability to capture potentially long-distance semantic characteristics [18]. However, the neighbor querying in feature domain almost completely ignores the geometric correlation in the original coordinate domain. For instance, in the shape of airplane, the points on the left engine may be aggregated with points on the right engine after feature domain queries, but the local geometry relationship between the left engine and wings may be ignored. To address this issue, we propose a Double K-nearest neighbor Feature Fusion (DKFF) for complementary fusion learning in both the coordinate and the feature domain.

Specifically, for each point in the point set, we use K-Nearest Neighbor (KNN) to construct local graphs in the spatial domain (i.e., the coordinate set  $X$ ) and feature domain

(i.e., the point features  $F$ ). Let  $x_i$  and  $f_j$  denotes the coordinate and corresponding feature of the  $i$ th point, respectively, then this process can be represented as:

$$\{x_i^j\}_{j=1}^K = KNN(x_i, X), \quad \{f_i^k\}_{k=1}^K = KNN(f_i, F) \quad (5)$$

Then, numerous critical elements in the local graph are identified and gathered to effectively aggregate features for  $i$ th point. Note that the aggregation in this stage is independently conducted for each spatial and feature domain. Take spatial domain as an example, we aggregate the direction vector  $(x_i - x_i^j)$ , feature subtraction offset  $(f_i - f_i^j)$ , inter-point distance  $\|x_i - x_i^j\|_2$ , and averaged feature distance  $L_i^j$  to characterize geometry dynamics  $p_i$  of the obtained spatial graph:

$$p_i = MLP \langle (x_i - x_i^j), (f_i - f_i^j), \|x_i - x_i^j\|_2, L_i^j \rangle \quad (6)$$

$$L_i^j = \frac{1}{C} \|f_i - f_i^j\|_1 \quad (7)$$

where  $\|\cdot\|_2$  represents the Euclidean distance between points,  $\langle \cdot \rangle$  represents the concatenate operation,  $\|\cdot\|_1$  represents the L1 norm,  $C$  refers to the channel dimension. Correspondingly, the feature dynamics  $q_i$  of the graph in the feature domain is expressed as:

$$q_i = MLP \langle (x_i - x_i^k), (f_i - f_i^k), \|x_i - x_i^k\|, L_i^k \rangle \quad (8)$$

$$L_i^k = \frac{1}{C} \|f_i - f_i^k\|_1 \quad (9)$$

We leverage the inverse bottleneck design [52], [53] to enrich feature extraction by expanding the output channels of hidden layer by 4 times in the subsequent MLP, as shown in Fig. 3. Then, maxpooling operation  $Max$  is used to aggregate the geometry features of each KNN graph to a feature vector:

$$P_i = Max(MLP(MLP(p_i))) \quad (10)$$

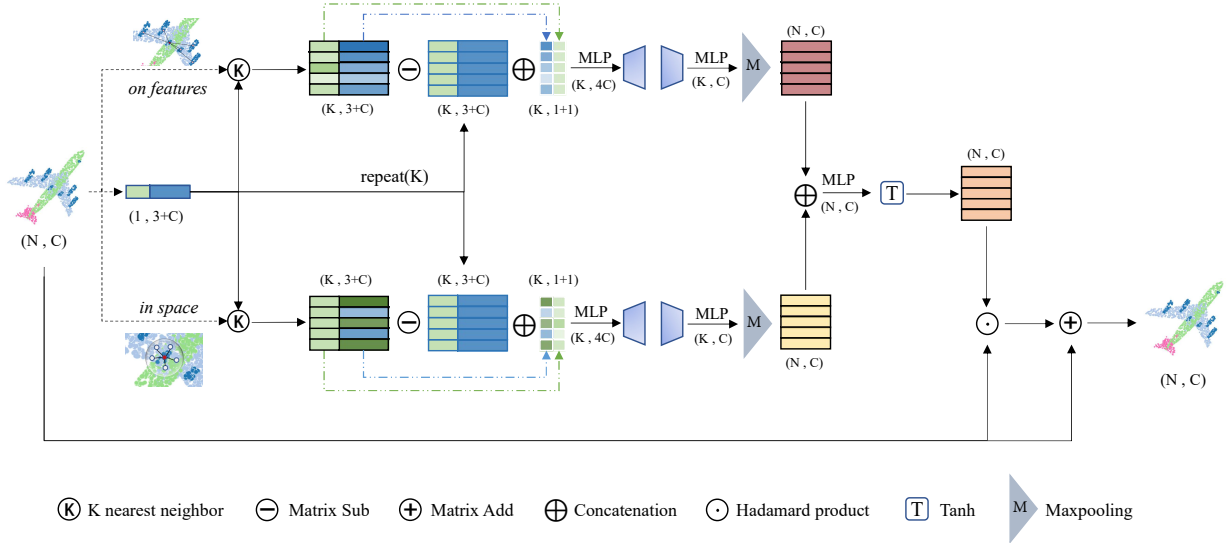


Fig. 3: Proposed Double K-nearest neighbor Feature Fusion (DKFF) module.  $N$  represents the number of points of the input point cloud;  $C$  denotes the dimension of feature channel; MLP means multilayer perceptron.

$$Q_i = \text{Max}(\text{MLP}(\text{MLP}(q_i))) \quad (11)$$

where  $P_i \in \mathbb{R}^{1 \times C}$  refers to the aggregated feature in the spatial domain and  $Q_i \in \mathbb{R}^{1 \times C}$  represents the feature in the feature domain. Here,  $P_i$  focuses on capturing geometry dynamics from spatial neighborhoods, whereas  $Q_i$  appreciates the feature-level neighbors that transcends spatial limitations, effectively complementing  $P_i$ .

To facilitate information exchange across different domains, we concatenate the aggregated feature of both domain, followed by a multilayer perceptron and a  $\text{Tanh}$  function to provide a residual multiplier  $W_i \in \mathbb{R}^{1 \times C}$ :

$$W_i = \text{Tanh}(\text{MLP}(\langle P_i, Q_i \rangle)) \quad (12)$$

where  $\langle \cdot \rangle$  represents the concatenate operation. The  $\text{Tanh}$  function, which manifests symmetry around the origin, restricting the obtained multiplier within the range of  $[-1, 1]$  to better serves for the subsequent multiplication. Let  $W \in \mathbb{R}^{N \times C}$  be the learned weight matrix that contains  $N$  residual multipliers (each multiplier corresponds to a point), we use Hadamard product to weight the input features by  $W$ , followed by a residual connection [30] to produce the output feature:

$$F_{out} = F_{in} \cdot W + F_{in} \quad (13)$$

The way of enhancing features through dual-domain aggregation and residual connections in the proposed DKFF module expands the receptive field of the neural network and mitigates the problem of gradient vanishing in deeply cascaded network modules. Beyond that, semantic information can be effectively exploited through interactive learning across different domains, which enhances the ability for point cloud understanding of the neural model.

#### IV. EXPERIMENTS

In section, we evaluate our method on multiple point cloud analysis tasks including classification, part segmentation,

and indoor large-scale semantic segmentation. State-of-the-art methods are compared for each task and extensive ablation studies are conducted to examine the effectiveness of our network structure.

##### A. Classification

**Data.** We use the ModelNet40 [31] and ScanObjectNN [32] datasets for point cloud classification evaluation. ModelNet40 [31] contains 12,311 meshed CAD models from 40 categories, of which 9,843 models are used for training and 2,468 models are used for testing. We follow the experimental setting of [17] and uniformly sample each object into 1,024 points containing only 3D coordinates as input. ScanObjectNN [32] contains about 15,000 real scanned objects which are further grouped into 15 classes with 2,902 unique object instances. Since point cloud samples in ScanObjectNN dataset are scanned from the real world, there exists noise caused by occlusion and missing background, which poses a major challenge to the existing point cloud analysis methods. It is also sampled into 1,024 points containing only three-dimensional coordinates as input.

**Network configuration.** Python and Pytorch is used to implement our model, and all experiments are conducted on two RTX 2080Ti GPUs. On ModelNet40 [31], the neighbor  $k$  value is selected as 16. Due to the noise in the ScanObjectNN [32] data, the  $k$  value is selected as 20, which is slightly larger. All layers use LeakyReLU and batch normalization. We use the SGD optimizer with momentum set to 0.9. The initial learning rate is 0.1 and reduced to 0.001 using cosine annealing. The batch size is set to 32. To prevent the network from overfitting, the random drop rate is set to 0.5, and the training is performed for 200 epochs. The data augmentation process all includes point displacement, scaling and perturbation.

**Results.** The classification results on ModelNet40 [31] are shown in Tab. I with the evaluation metrics of mean class accuracy (mAcc) and overall accuracy (OA). The input data format and number of points are also provided for a detailed



comparison. It can be seen that our method achieves the best performance on overall accuracy using only 1k points containing 3D coordinates, which is significantly better than other methods. Note that the latest published works are also included, such as M-GCN [54], PointConT [55], IBT [20], OctFormer [16], and PointMamba [21].

TABLE I: Classification results on ModelNet40.

Methods	Input	point	mAcc	OA
<b>Other Learning-based Methods</b>				
Pointnet [17]	xyz	1k	86.0	89.2
Pointnet++ [23]	xyz,normal	5k	-	91.9
PointCNN [56]	xyz	1k	88.1	92.2
DGCNN [18]	xyz	1k	90.2	92.2
SpiderCNN [57]	xyz,normal	1k	-	92.4
PointWeb [58]	xyz,normal	1k	89.4	92.3
PointConv [45]	xyz,normal	1k	-	92.5
Point2Sequence [59]	xyz	1k	90.4	92.6
KPCConv [44]	xyz	6k	-	92.9
FPCConv [60]	xyz,normal	1k	-	92.5
Point2Node [61]	xyz	1k	-	93.0
M-GCN [54]	xyz	1k	90.1	93.1
AG-conv [27]	xyz	1k	90.7	93.4
PointStack [62]	xyz	1k	89.6	93.3
PointMamba [21]	xyz	1k	-	92.4
<b>Transformer-based Methods</b>				
A-SCN [63]	xyz	1k	87.6	90.0
PATs [64]	xyz	1k	-	91.7
GAPNet [65]	xyz,normal	1k	89.7	92.4
LFT-Net [66]	xyz,normal	2k	89.7	93.2
3DETR [67]	xyz	1k	89.9	91.9
MLMST [68]	xyz	1k	-	92.9
PCT [28]	xyz	1k	-	93.2
CloudTransformers [69]	xyz	1k	90.8	93.1
3DCTN [63]	xyz,normal	1k	91.2	93.3
PointASNL [50]	xyz	1k	-	92.9
PointASNL [50]	xyz,normal	1k	-	93.2
PT [19]	xyz,normal	1k	90.6	93.7
PointConT [55]	xyz	1k	-	93.5
IBT [20]	xyz	1k	91.0	93.6
OctFormer [16]	xyz	1k	-	92.7
Ours	xyz	1k	91.1	<b>93.8</b>

Tab. II shows the classification results on ScanObjectNN dataset [32], where our method continues to provide superior classification performance. Due to the defect of the objects within this dataset such as occlusion and noise, this also proves the significant stability and robustness of our method.

TABLE II: Classification results on ScanObjectNN.

Methods	mAcc	OA
3DmFV [70]	58.1	63.0
Pointnet [17]	63.4	68.2
Spiderncn [57]	69.8	73.7
Pointnet++ [23]	75.4	77.9
DGCNN [18]	73.6	78.1
PointCNN [56]	75.1	78.5
BGA-DGCNN [32]	75.7	79.7
BGA-PN++ [32]	77.5	80.2
DRNet [71]	78.0	80.3
GBNet [72]	77.8	80.5
SimpleView [73]	-	80.5
PRANet [74]	79.1	82.1
PointMamba [21]	-	82.5
Ours	<b>80.1</b>	<b>82.6</b>

### B. Part segmentation

**Data.** We further test our model on the part segmentation task on the ShapeNetPart [33] dataset. The dataset contains 16,880 shapes from 16 categories, of which 14,006 are used for training and 2,874 are used for testing. The number of parts in each category ranges from 2 to 6, for a total of 50 different

parts. We follow the experimental setup of [23], but only sample 1,024 points from each shape instead of 2,048. Our input data include only 3D coordinates and no point normal is attached.

**Network configuration.** Following [18], we include a one-hot vector representing category types for each point. We concatenate the high-dimensional global feature vector obtained in the classification task and categorical vector with the previously learned semantic features of different levels to predict the category of each point. The settings of other training parameters are the same as our classification task, except that the neighbor value  $k$  is set to 40 to further expand the receptive field to learn fine-grained features.

**Results.** Tab. III reports the part segmentation results of different methods, where we use the mean class IoU (mIoU) per class and mean instance IoU (mIoU) across all shapes in all categories as metrics. Note that the IoU of a shape is computed by averaging the IoU of each part and the mIoU is computed by averaging the IoUs of all testing instances. Our method performs better on most categories and also performs well in terms of overall mIoU. In addition, we also have a visual comparison of part segmentation with some other mainstream methods, as shown in Fig. 4. For parts such as aircraft wing engines, rocket heads and tails, guitar strings, etc., our method is significantly closer to the ground truth.

### C. Indoor scene segmentation

**Data.** We further test the semantic segmentation performance on the large-scale dataset S3DIS [34] which contains 3D RGB point clouds of six indoor areas from three different buildings with a total of 271 rooms. Each point is annotated with a semantic label from 13 categories. We follow the experimental settings of [18] to divide the original large-scale point cloud data into  $1m \times 1m$  blocks, and randomly sample 4,096 points within each block. Each block is then treated as independent input for the neural network. The attributes of the input point include coordinates, color, and normalized spatial coordinates. We choose Area 5 as the test set which is not in the same building as other areas.

**Network configuration.** The training parameters and network structure are the same as the part segmentation, but no additional class vectors are introduced. Given the increased complexity involved in large-scale semantic segmentation task, we increased the stack depth of the DKFF module to 5 layers to encourage the network to learn richer semantic features.

**Results.** We report the mIoU, mean classwise accuracy (mAcc) and overall accuracy (OA) in Tab. IV and provide visualization results in Fig. 5. As seen, our method slightly underperforms the state of the arts but there exists reasons for this issue. The primary factor, we believe, lies in the necessity to reduce the input size to  $1m \times 1m$  blocks with merely 4k points, to fit the limited hardware resource. In contrast, previous works [25], [19], [78], [27] usually input more points even the entire scenes for training due to their ample computational resources.

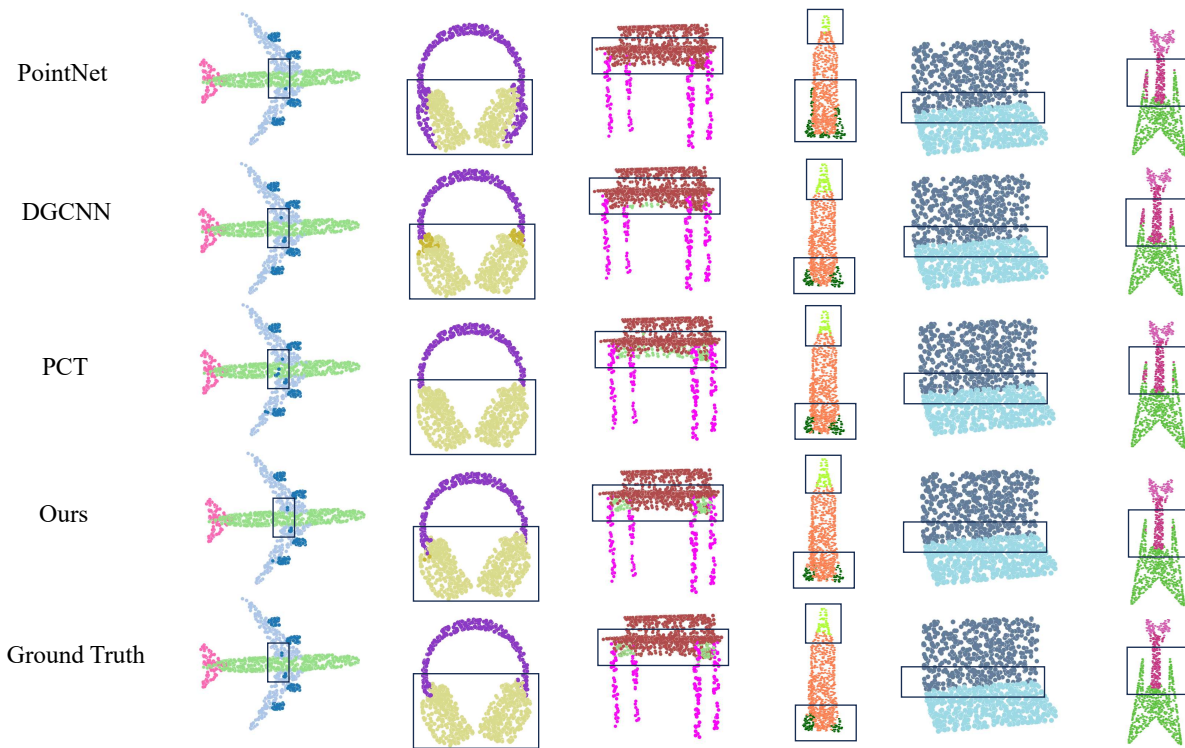


Fig. 4: Visual comparison with other methods for part segmentation.

TABLE III: Part segmentation results on ShapeNet dataset. Metric is mIoU(%).

Methods	mIoU	air.	bag	cap	car	cha.	ear.	gui.	kni.	lam.	lap.	mot.	mug	pis.	roc.	ska.	tab.
NUM		2690	76	55	898	3758	69	787	392	1547	451	202	184	283	66	152	5271
Other Learning-based Methods																	
Pointnet [17]	83.7	83.4	78.7	82.5	74.9	89.6	73.0	91.5	85.9	80.8	95.3	65.2	93.0	81.2	57.9	72.8	80.6
Pointnet++ [23]	85.1	82.4	79.0	87.7	77.3	90.8	71.8	91.0	85.9	83.7	95.3	71.6	94.1	81.3	58.7	76.4	82.6
RGCNN [26]	84.3	80.2	82.8	<b>92.6</b>	75.3	89.2	73.7	91.3	88.4	83.3	96.0	63.9	95.7	60.9	44.6	72.9	80.4
<b>SO-Net</b> [75]	84.9	82.8	77.8	88.0	77.3	90.6	73.5	90.7	83.9	82.8	94.8	69.1	94.2	80.9	53.1	72.9	83.0
DGCNN [18]	85.2	84.0	83.4	86.7	77.8	90.6	74.7	91.2	87.5	82.8	95.7	66.3	94.9	81.1	63.5	74.5	82.6
PCNN [46]	85.1	82.4	80.1	85.5	79.5	90.8	73.2	91.3	86.0	85.0	96.7	73.2	94.8	83.3	51.0	75.0	81.8
3D-GCN [76]	85.1	83.1	84.0	86.6	77.5	90.3	74.1	90.9	86.4	83.8	95.3	65.2	93.0	81.2	59.6	75.7	82.8
PointMamba [21]	85.8	-	-	-	-	-	-	-	-	-	-	-	-	-	-	-	-
Transformer-based Methods																	
<b>A-SCN</b> [63]	84.6	83.8	80.8	83.5	79.3	90.5	69.8	91.7	86.5	82.9	96.0	69.2	93.8	82.5	62.9	74.4	80.8
<b>GAPNet</b> [65]	84.7	84.2	84.1	88.8	78.1	90.7	70.1	91.0	87.3	83.1	96.2	65.9	95.0	81.7	60.7	74.9	80.8
MLMST [68]	86.0	83.6	<b>84.7</b>	86.3	79.8	91.1	71.2	90.2	<b>88.6</b>	84.9	95.9	72.8	94.8	83.4	56.2	76.7	82.6
PointASNL [50]	86.1	84.1	<b>84.7</b>	87.9	79.7	<b>92.2</b>	73.7	91.0	87.2	84.2	95.8	74.4	<b>95.2</b>	81.0	63.0	76.3	83.2
PCT [28]	86.4	85.0	82.4	89.0	<b>81.2</b>	91.9	71.5	91.3	88.1	<b>86.3</b>	95.8	64.6	<b>95.8</b>	83.6	62.2	<b>77.6</b>	83.7
Point2Vec [77]	86.3	-	-	-	-	-	-	-	-	-	-	-	-	-	-	-	-
IBT [20]	86.2	85.2	81.4	86.1	80.1	91.5	<b>76.6</b>	<b>91.9</b>	87.6	84.6	<b>97.1</b>	72.9	95.4	84.3	<b>63.7</b>	76.5	83.9
Ours	86.3	<b>85.4</b>	82.0	84.0	80.8	91.2	76.5	<b>92.0</b>	87.7	85.3	96.2	<b>74.8</b>	95.2	<b>84.8</b>	63.5	75.5	<b>84.0</b>

TABLE IV: Segmentation results on S3DIS.

Methods	mAcc	OA	mIoU
Pointnet [17]	49.0	-	41.1
SEGCloud [79]	57.3	-	48.9
RSNet [80]	57.3	-	51.9
PointCNN [56]	63.9	85.9	57.3
PointWeb [58]	66.6	86.9	60.3
SPG [81]	66.5	86.4	58.0
ELGS [82]	-	88.4	60.1
Grid-GCN [83]	87.0	86.9	57.8
PCT [28]	67.6	-	61.3
PointASNL [50]	68.5	87.7	62.6
Ours	68.5	88.3	62.9

#### D. Ablation experiment

In this subsection, we explore additional architectural choices of the network and conduct ablation studies on the proposed modules.

**Efficacy of proposed modules.** We design the Contextual Position-enhanced Transformer (CPT) to produce a global-

aware input embedding that serves as the guidance to subsequent aggregations and facilitates network learning. This has not been previously investigated and differs from existing methods that directly map 3D coordinates to higher dimensions to obtain initial features. To validate the efficacy of this module, we conduct ablation study by replacing the CPT module with conventional shared MLP to obtain the initial features.

The Double K-nearest neighbor Feature Fusion (DKFF) module provides highly effective feature aggregation by conducting novel dual-domain feature learning. In this subsection, we evaluated the model's performance in single domain, either spatial or feature domain, to examine the efficiency of proposed dual-domain learning.

Results of this ablation study on 1k points ModelNet40 [31] are shown in Tab. V, where  $\checkmark$  means to keep the module, and blank means to remove it. It can be seen that the way of



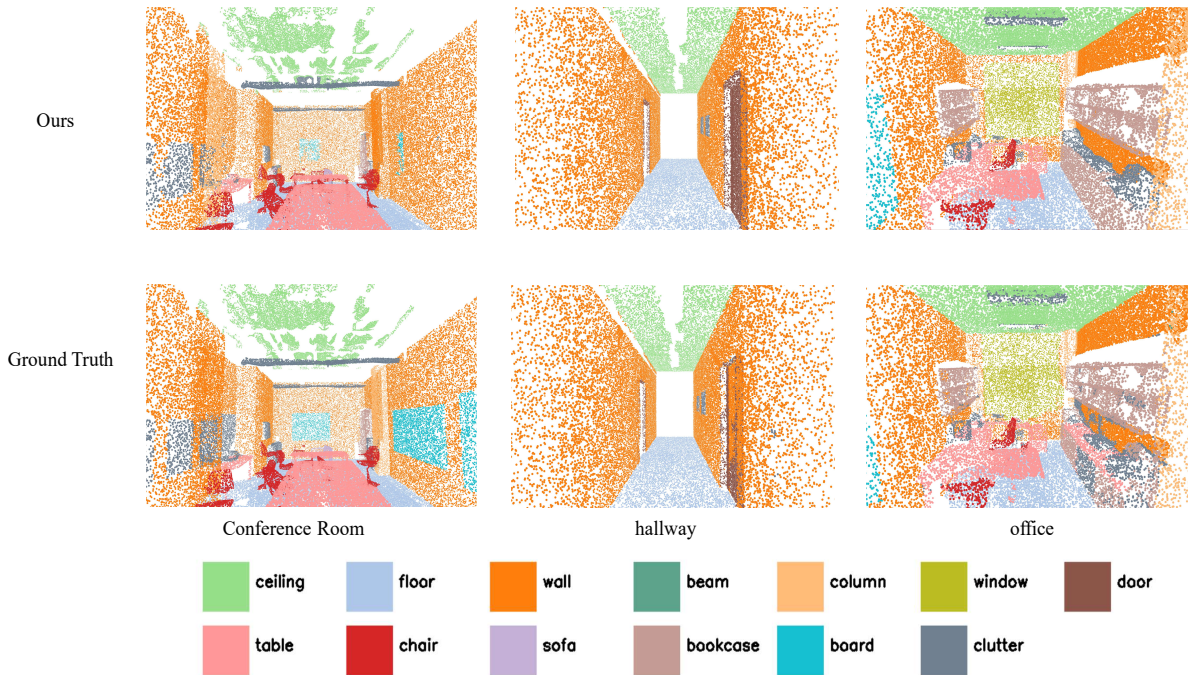


Fig. 5: Visualization of semantic segmentation results on the S3DIS dataset.

expanding the receptive field with dual domains is efficient, and the best performance can be obtained with the initial features enhanced by CPT.

TABLE V: Ablation experiments for the proposed CPT and DKFF modules. Classification task is considered as the benchmark task.

Model	CPT	DKFF (in space)	DKFF (in feature)	mAcc	OA
Baseline (PointNet)				86.0	89.2
A	✓	✓		90.5	93.3
B	✓		✓	90.7	93.4
C		✓	✓	90.4	93.4
D	✓	✓	✓	<b>91.1</b>	<b>93.8</b>

**Module designing.** We perform investigations into the specifics of the design of proposed CPT and DKFF modules, the results are shown in Tab. VI. Several interesting phenomenons can be observed. First, the aim of adding Euclidean distance and feature average metric is to learn complex geometric patterns, which is more helpful for original noise-free data sets such as ModelNet40 [31] and ShapeNetPart [33]. But for the noisy samples in ScanObjectNN [32], this scheme appears ineffective since the aforementioned auxiliaries introduces interference information on noisy inputs. Second, learning from self-attention is relatively more fragile and less efficient than offset attention. Third, the fusion of location information and attention weights performs much better than that of ignoring location information, which fully proves the importance of location information for subsequent point cloud learning.

**Number of DKFF layer.** We conduct ablation experiments to verify the impact of the number of cascaded DKFF layers. We retrain our network under four different conditions (i.e., 1~4 layers) and test it using classification benchmarks. Results of this ablation study on 1k points ModelNet40 [31] are shown

TABLE VI: Ablation experiments for different options within the module.

Module		ModelNet40	ScanObjectNN
CPT	w/o $bias_X$	93.2	81.2
	use $P_X$ instead of $bias_X$	93.4	81.8
	use SA instead of offset attention	93.0	80.3
DKFF	w/o distance and feature averaging metric	93.6	<b>82.6</b>
	use average pooling instead of maxpooling	93.2	81.3
	use attention pooling instead of maxpooling	93.2	80.9
	use Sigmoid instead of Tanh	93.5	82.2
both		<b>93.8</b>	81.8

in Tab. VII. As seen, increasing the depth of stacked layers generally yields improved performance. However, excessively deep structures (e.g., four or more layers) can hinder network learning due to an increase in the number of parameters that require optimization, potentially leading to suboptimal convergence.

TABLE VII: Ablation study for the number of cascaded DKFF layers. Classification task is considered as the benchmark task.

Number of DKFF layer	mAcc	OA
1	90.5	93.2
2	90.8	93.5
3	<b>91.1</b>	<b>93.8</b>
4	91.0	93.6

**k-nearest neighbor value.** Considering the strong association between the feature aggregation efficiency and receptive field size, which is determined by the value k of the KNN gathering in the DKFF module, we conduct ablation experiments to assess the network performance across different k values. As seen in Tab. VIII, a small k value leads to inadequate information exchange within neighboring points, while a large k value may exert complex context patterns, diminishing prediction accuracy. We consider 16~20 as appropriate values for sparse point cloud samples.

TABLE VIII: Ablation study for different k values of the DKFF module. Overall accuracy (OA) for classification benchmark datasets (i.e., ModelNet40 and ScanObjectNN) is reported.

k value	ModelNet40	ScanObjectNN
8	92.8	79.5
12	93.3	80.7
16	<b>93.8</b>	81.4
20	93.6	<b>82.6</b>
24	93.4	81.9

## V. CONCLUSION

In this paper, we propose a novel global attention-guided dual-domain feature learning network for 3D point clouds. The main contribution of our method lies in the design of the Contextual Position-enhanced Transformer module (CPT) and the Double K-nearest neighbor Feature Fusion (DKFF) module. The CPT module produce a global-aware input embedding that serves as the guidance to subsequent aggregations and facilitates network learning. The DKFF module dynamically constructs graphs in dual domains, which appreciates both local geometric relations and long-distance semantic connections, provides highly effective feature aggregation. The proposed network can be trained in an end-to-end fashion and demonstrates superior performance on various point cloud analysis tasks, including classification, part segmentation, and large-scale semantic segmentation. Moreover, the proposed modules are ready to serve as plug-and-play blocks for downstream tasks such as completion, denoising, and compression.

## REFERENCES

- [1] J. Zhang, F. Zhang, S. Kuang, and L. Zhang, "Nerf-lidar: Generating realistic lidar point clouds with neural radiance fields," in *Proceedings of the AAAI Conference on Artificial Intelligence*, vol. 38, no. 7, 2024, pp. 7178–7186.
- [2] S. Tang, G. Wang, Q. Ran, L. Li, L. Shen, and P. Tan, "High-resolution volumetric reconstruction for clothed humans," *ACM Trans. Graph.*, vol. 42, no. 5, aug 2023. [Online]. Available: <https://doi.org/10.1145/3606032>
- [3] W. Fang, L. Chen, T. Zhang, C. Chen, Z. Teng, and L. Wang, "Head-mounted display augmented reality in manufacturing: A systematic review," *Robotics and Computer-Integrated Manufacturing*, vol. 83, p. 102567, 2023.
- [4] J. Mao, S. Shi, X. Wang, and H. Li, "3d object detection for autonomous driving: A comprehensive survey," *International Journal of Computer Vision*, vol. 131, no. 8, pp. 1909–1963, 2023.
- [5] D. Graziosi, O. Nakagami, S. Kuma, A. Zaghetto, T. Suzuki, and A. Tabatabai, "An overview of ongoing point cloud compression standardization activities: Video-based (v-pcc) and geometry-based (g-pcc)," *APSIPA Transactions on Signal and Information Processing*, vol. 9, p. e13, 2020.
- [6] P. S. Chib and P. Singh, "Recent advancements in end-to-end autonomous driving using deep learning: A survey," *IEEE Transactions on Intelligent Vehicles*, 2023.
- [7] A. Xiao, J. Huang, D. Guan, X. Zhang, S. Lu, and L. Shao, "Unsupervised point cloud representation learning with deep neural networks: A survey," *IEEE Transactions on Pattern Analysis and Machine Intelligence*, vol. 45, no. 9, pp. 11 321–11 339, 2023.
- [8] Z. Zhuang, Z. Zhi, T. Han, Y. Chen, J. Chen, C. Wang, M. Cheng, X. Zhang, N. Qin, and L. Ma, "A survey of point cloud completion," *IEEE Journal of Selected Topics in Applied Earth Observations and Remote Sensing*, vol. 17, pp. 5691–5711, 2024.
- [9] F. J. Lawin, M. Danelljan, P. Tosteborg, G. Bhat, F. S. Khan, and M. Felsberg, "Deep projective 3d semantic segmentation," in *International Conference on Computer Analysis of Images and Patterns*. Springer, 2017, pp. 95–107.
- [10] Z. Yang and L. Wang, "Learning relationships for multi-view 3d object recognition," in *Proceedings of the IEEE/CVF International Conference on Computer Vision*, 2019, pp. 7505–7514.
- [11] A. Hamdi, S. Giancola, and B. Ghanem, "Mvtn: Multi-view transformation network for 3d shape recognition," in *Proceedings of the IEEE/CVF International Conference on Computer Vision*, 2021, pp. 1–11.
- [12] X. Ning, Z. Yu, L. Li, W. Li, and P. Tiwari, "Dilf: Differentiable rendering-based multi-view image–language fusion for zero-shot 3d shape understanding," *Information Fusion*, vol. 102, p. 102033, 2024.
- [13] C. R. Qi, H. Su, M. Nießner, A. Dai, M. Yan, and L. J. Guibas, "Volumetric and multi-view cnns for object classification on 3d data," in *Proceedings of the IEEE conference on computer vision and pattern recognition*, 2016, pp. 5648–5656.
- [14] H.-Y. Meng, L. Gao, Y.-K. Lai, and D. Manocha, "Vv-net: Voxel vae net with group convolutions for point cloud segmentation," in *Proceedings of the IEEE/CVF international conference on computer vision*, 2019, pp. 8500–8508.
- [15] C. Zhang, H. Wan, X. Shen, and Z. Wu, "Pvt: Point-voxel transformer for point cloud learning," *International Journal of Intelligent Systems*, vol. 37, no. 12, pp. 11 985–12 008, 2022.
- [16] P.-S. Wang, "Octformer: Octree-based transformers for 3d point clouds," *ACM Trans. Graph.*, vol. 42, no. 4, jul 2023. [Online]. Available: <https://doi.org/10.1145/3592131>
- [17] C. R. Qi, H. Su, K. Mo, and L. J. Guibas, "Pointnet: Deep learning on point sets for 3d classification and segmentation," in *Proceedings of CVPR*, 2017, pp. 652–660.
- [18] Y. Wang, Y. Sun, Z. Liu, S. E. Sarma, M. M. Bronstein, and J. M. Solomon, "Dynamic graph cnn for learning on point clouds," *Acm Transactions On Graphics*, vol. 38, no. 5, pp. 1–12, 2019.
- [19] H. Zhao, L. Jiang, J. Jia, P. H. Torr, and V. Koltun, "Point transformer," in *Proceedings of ICCV*, 2021, pp. 16 259–16 268.
- [20] Z. Li, P. Gao, H. Yuan, R. Wei, and M. Paul, "Exploiting inductive bias in transformer for point cloud classification and segmentation," in *2023 IEEE International Conference on Multimedia and Expo Workshops (ICMEW)*. IEEE, 2023, pp. 140–145.
- [21] D. Liang, X. Zhou, X. Wang, X. Zhu, W. Xu, Z. Zou, X. Ye, and X. Bai, "Pointmamba: A simple state space model for point cloud analysis," *arXiv preprint arXiv:2402.10739*, 2024.
- [22] B. Liu, M. Wang, H. Foroosh, M. Tappen, and M. Pensky, "Sparse convolutional neural networks," in *2015 IEEE Conference on Computer Vision and Pattern Recognition (CVPR)*, 2015, pp. 806–814.
- [23] C. R. Qi, L. Yi, H. Su, and L. J. Guibas, "Pointnet++: Deep hierarchical feature learning on point sets in a metric space," *NIPS*, vol. 30, 2017.
- [24] X. Wu, Y. Lao, L. Jiang, X. Liu, and H. Zhao, "Point transformer v2: Grouped vector attention and partition-based pooling," in *NeurIPS*, 2022.
- [25] Q. Hu, B. Yang, L. Xie, S. Rosa, Y. Guo, Z. Wang, N. Trigoni, and A. Markham, "Randla-net: Efficient semantic segmentation of large-scale point clouds," in *Proceedings of CVPR*, 2020, pp. 11 108–11 117.
- [26] G. Te, W. Hu, A. Zheng, and Z. Guo, "Rgcnn: Regularized graph cnn for point cloud segmentation," in *Proceedings of the 26th ACM Multimedia*, 2018, pp. 746–754.
- [27] H. Zhou *et al.*, "Adaptive graph convolution for point cloud analysis," in *Proceedings of the IEEE/CVF International Conference on Computer Vision*, 2021, pp. 4965–4974.
- [28] M.-H. Guo, J.-X. Cai, Z.-N. Liu, T.-J. Mu, R. R. Martin, and S.-M. Hu, "PCT: Point cloud transformer," *Computational Visual Media*, vol. 7, no. 2, pp. 187–199, 2021.
- [29] W. Han, H. Wu, C. Wen, C. Wang, and X. Li, "Blnet: Bidirectional learning network for point clouds," *Computational Visual Media*, pp. 1–12, 2022.
- [30] K. He, X. Zhang, S. Ren, and J. Sun, "Deep residual learning for image recognition," in *Proceedings of the IEEE conference on computer vision and pattern recognition*, 2016, pp. 770–778.
- [31] Z. Wu, S. Song, A. Khosla, F. Yu, L. Zhang, X. Tang, and J. Xiao, "3D shapenets: A deep representation for volumetric shapes," in *Proceedings of CVPR*, 2015, pp. 1912–1920.
- [32] M. A. Uy, Q.-H. Pham, B.-S. Hua, T. Nguyen, and S.-K. Yeung, "Revisiting point cloud classification: A new benchmark dataset and classification model on real-world data," in *Proceedings of ICCV*, 2019, pp. 1588–1597.
- [33] L. Yi *et al.*, "A scalable active framework for region annotation in 3d shape collections," *ACM Transactions on Graphics (ToG)*, vol. 35, no. 6, pp. 1–12, 2016.
- [34] I. Armeni, O. Sener, A. R. Zamir, H. Jiang, I. Brilakis, M. Fischer, and S. Savarese, "3d semantic parsing of large-scale indoor spaces," in *Proceedings of the IEEE conference on computer vision and pattern recognition*, 2016, pp. 1534–1543.

- [35] H. Su, S. Maji, E. Kalogerakis, and E. Learned-Miller, "Multi-view convolutional neural networks for 3d shape recognition," in *Proceedings of the IEEE international conference on computer vision*, 2015, pp. 945–953.
- [36] T. Yu, J. Meng, and J. Yuan, "Multi-view harmonized bilinear network for 3d object recognition," in *Proceedings of the IEEE conference on computer vision and pattern recognition*, 2018, pp. 186–194.
- [37] X. Wei, R. Yu, and J. Sun, "View-gcn: View-based graph convolutional network for 3d shape analysis," in *Proceedings of the IEEE/CVF Conference on Computer Vision and Pattern Recognition*, 2020, pp. 1850–1859.
- [38] G. Riegler, A. Osman Ulusoy, and A. Geiger, "Octnet: Learning deep 3d representations at high resolutions," in *Proceedings of the IEEE conference on computer vision and pattern recognition*, 2017, pp. 3577–3586.
- [39] P.-S. Wang, Y. Liu, Y.-X. Guo, C.-Y. Sun, and X. Tong, "O-cnn: Octree-based convolutional neural networks for 3d shape analysis," *ACM Transactions On Graphics (TOG)*, vol. 36, no. 4, pp. 1–11, 2017.
- [40] T. Le and Y. Duan, "Pointgrid: A deep network for 3d shape understanding," in *Proceedings of the IEEE conference on computer vision and pattern recognition*, 2018, pp. 9204–9214.
- [41] Y. Ben-Shabat, M. Lindenbaum, and A. Fischer, "3d point cloud classification and segmentation using 3d modified fisher vector representation for convolutional neural networks," *arXiv preprint arXiv:1711.08241*, 2017.
- [42] Y. Duan, Y. Zheng, J. Lu, J. Zhou, and Q. Tian, "Structural relational reasoning of point clouds," in *Proceedings of the IEEE/CVF Conference on Computer Vision and Pattern Recognition*, 2019, pp. 949–958.
- [43] Y. Liu, B. Fan, S. Xiang, and C. Pan, "Relation-shape convolutional neural network for point cloud analysis," in *Proceedings of the IEEE/CVF Conference on Computer Vision and Pattern Recognition*, 2019, pp. 8895–8904.
- [44] H. Thomas *et al.*, "Kpconv: Flexible and deformable convolution for point clouds," in *Proceedings of the IEEE/CVF international conference on computer vision*, 2019, pp. 6411–6420.
- [45] W. Wu, Z. Qi, and L. Fuxin, "Pointconv: Deep convolutional networks on 3d point clouds," in *Proceedings of CVPR*, 2019, pp. 9621–9630.
- [46] M. Atzmon, H. Maron, and Y. Lipman, "Point convolutional neural networks by extension operators," *arXiv preprint arXiv:1803.10091*, 2018.
- [47] M. Simonovsky and N. Komodakis, "Dynamic edge-conditioned filters in convolutional neural networks on graphs," in *Proceedings of the IEEE conference on computer vision and pattern recognition*, 2017, pp. 3693–3702.
- [48] Y. Shen, C. Feng, Y. Yang, and D. Tian, "Mining point cloud local structures by kernel correlation and graph pooling," in *Proceedings of the IEEE conference on computer vision and pattern recognition*, 2018, pp. 4548–4557.
- [49] Y. Zhang and M. Rabbat, "A graph-cnn for 3d point cloud classification," in *2018 IEEE International Conference on Acoustics, Speech and Signal Processing (ICASSP)*. IEEE, 2018, pp. 6279–6283.
- [50] X. Yan, C. Zheng, Z. Li, S. Wang, and S. Cui, "Pointasnl: Robust point clouds processing using nonlocal neural networks with adaptive sampling," in *Proceedings of the CVPR*, 2020, pp. 5589–5598.
- [51] C. Zhang, H. Wan, X. Shen, and Z. Wu, "Pvt: Point-voxel transformer for point cloud learning," *arXiv preprint arXiv:2108.06076*, 2021.
- [52] G. Qian, Y. Li, H. Peng, J. Mai, H. Hammoud, M. Elhoseiny, and B. Ghanem, "Pointnext: Revisiting pointnet++ with improved training and scaling strategies," *Advances in Neural Information Processing Systems*, vol. 35, pp. 23 192–23 204, 2022.
- [53] M. Sandler, A. Howard, M. Zhu, A. Zhmoginov, and L.-C. Chen, "Mobilenetv2: Inverted residuals and linear bottlenecks," in *Proceedings of the IEEE conference on computer vision and pattern recognition*, 2018, pp. 4510–4520.
- [54] J. Hu, X. Wang, Z. Liao, and T. Xiao, "M-gcn: Multi-scale graph convolutional network for 3d point cloud classification," in *2023 IEEE International Conference on Multimedia and Expo (ICME)*. IEEE, 2023, pp. 924–929.
- [55] Y. Liu, B. Tian, Y. Lv, L. Li, and F.-Y. Wang, "Point cloud classification using content-based transformer via clustering in feature space," *IEEE/CAA Journal of Automatica Sinica*, 2023.
- [56] Y. Li, R. Bu, M. Sun, W. Wu, X. Di, and B. Chen, "Pointcnn: Convolution on x-transformed points," *Advances in neural information processing systems*, vol. 31, 2018.
- [57] Y. Xu, T. Fan, M. Xu, L. Zeng, and Y. Qiao, "Spidercnn: Deep learning on point sets with parameterized convolutional filters," in *Proceedings of the European Conference on Computer Vision (ECCV)*, 2018, pp. 87–102.
- [58] H. Zhao, L. Jiang, C.-W. Fu, and J. Jia, "Pointweb: Enhancing local neighborhood features for point cloud processing," in *Proceedings of CVPR*, 2019, pp. 5565–5573.
- [59] X. Liu, Z. Han, Y.-S. Liu, and M. Zwicker, "Point2sequence: Learning the shape representation of 3d point clouds with an attention-based sequence to sequence network," in *Proceedings of the AAAI Conference on Artificial Intelligence*, vol. 33, no. 01, 2019, pp. 8778–8785.
- [60] Y. Lin *et al.*, "Fpconv: Learning local flattening for point convolution," in *Proceedings of CVPR*, 2020, pp. 4293–4302.
- [61] W. Han, C. Wen, C. Wang, X. Li, and Q. Li, "Point2node: Correlation learning of dynamic-node for point cloud feature modeling," in *Proceedings of the AAAI Conference on Artificial Intelligence*, vol. 34, no. 07, 2020, pp. 10925–10932.
- [62] K. T. Wijaya, D.-H. Paek, and S.-H. Kong, "Advanced feature learning on point clouds using multi-resolution features and learnable pooling," *arXiv preprint arXiv:2205.09962*, 2022.
- [63] S. Xie, S. Liu, Z. Chen, and Z. Tu, "Attentional shapecontextnet for point cloud recognition," in *Proceedings of CVPR*, 2018, pp. 4606–4615.
- [64] J. Yang, Q. Zhang, B. Ni, L. Li, J. Liu, M. Zhou, and Q. Tian, "Modeling point clouds with self-attention and gumbel subset sampling," in *Proceedings of the IEEE/CVF conference on computer vision and pattern recognition*, 2019, pp. 3323–3332.
- [65] C. Chen, L. Z. Fragonara, and A. Tsourdos, "Gapnet: Graph attention based point neural network for exploiting local feature of point cloud," *arXiv preprint arXiv:1905.08705*, 2019.
- [66] Y. Gao, X. Liu, J. Li, Z. Fang, X. Jiang, and K. M. S. Huq, "Lft-net: Local feature transformer network for point clouds analysis," *IEEE transactions on intelligent transportation systems*, 2022.
- [67] I. Misra, R. Girdhar, and A. Joulin, "An end-to-end transformer model for 3d object detection," in *Proceedings of the IEEE/CVF International Conference on Computer Vision*, 2021, pp. 2906–2917.
- [68] Q. Zhong and X.-F. Han, "Point cloud learning with transformer," *arXiv preprint arXiv:2104.13636*, 2021.
- [69] K. Mazur and V. Lempitsky, "Cloud transformers: A universal approach to point cloud processing tasks," in *Proceedings of ICCV*, 2021, pp. 10 715–10 724.
- [70] Y. Ben-Shabat, M. Lindenbaum, and A. Fischer, "3dmfv: Three-dimensional point cloud classification in real-time using convolutional neural networks," *IEEE Robotics and Automation Letters*, vol. 3, no. 4, pp. 3145–3152, 2018.
- [71] S. Qiu, S. Anwar, and N. Barnes, "Dense-resolution network for point cloud classification and segmentation," in *Proceedings of WCAV*, 2021, pp. 3813–3822.
- [72] —, "Geometric back-projection network for point cloud classification," *IEEE TMM*, vol. 24, pp. 1943–1955, 2021.
- [73] A. Goyal, H. Law, B. Liu, A. Newell, and J. Deng, "Revisiting point cloud shape classification with a simple and effective baseline," in *ICML*, 2021, pp. 3809–3820.
- [74] S. Cheng, X. Chen, X. He, Z. Liu, and X. Bai, "Pra-net: Point relation-aware network for 3d point cloud analysis," *IEEE TIP*, vol. PP, no. 99, 2021.
- [75] J. Li, B. M. Chen, and G. H. Lee, "So-net: Self-organizing network for point cloud analysis," in *Proceedings of the IEEE conference on computer vision and pattern recognition*, 2018, pp. 9397–9406.
- [76] Z.-H. Lin, S.-Y. Huang, and Y.-C. F. Wang, "Convolution in the cloud: Learning deformable kernels in 3d graph convolution networks for point cloud analysis," in *Proceedings of the CVPR*, 2020, pp. 1800–1809.
- [77] K. Abou Zeid, J. Schult, A. Hermans, and B. Leibe, "Point2vec for self-supervised representation learning on point clouds," *arXiv e-prints*, pp. arXiv–2303, 2023.
- [78] X. Lai, J. Liu, L. Jiang, L. Wang, H. Zhao, S. Liu, X. Qi, and J. Jia, "Stratified transformer for 3d point cloud segmentation," in *Proceedings of the IEEE/CVF Conference on Computer Vision and Pattern Recognition*, 2022, pp. 8500–8509.
- [79] L. Tchapmi, C. Choy, I. Armeni, J. Gwak, and S. Savarese, "Segcloud: Semantic segmentation of 3d point clouds," in *2017 international conference on 3D vision (3DV)*. IEEE, 2017, pp. 537–547.
- [80] Q. Huang, W. Wang, and U. Neumann, "Recurrent slice networks for 3d segmentation of point clouds," in *Proceedings of the IEEE conference on computer vision and pattern recognition*, 2018, pp. 2626–2635.
- [81] L. Landrieu and M. Simonovsky, "Large-scale point cloud semantic segmentation with superpoint graphs," in *Proceedings of the IEEE conference on computer vision and pattern recognition*, 2018, pp. 4558–4567.

- [82] X. Wang, J. He, and L. Ma, “Exploiting local and global structure for point cloud semantic segmentation with contextual point representations,” *Advances in Neural Information Processing Systems*, vol. 32, 2019.
- [83] Q. Xu, X. Sun, C.-Y. Wu, P. Wang, and U. Neumann, “Grid-gcn for fast and scalable point cloud learning,” in *Proceedings of the IEEE/CVF Conference on Computer Vision and Pattern Recognition*, 2020, pp. 5661–5670.